Sorbent-based Oxygen Separation with YBC114 for Energy Storage Systems

Mai Xu [a,b], *Ivan Ermanoski* [b], *Ellen B. Stechel* [c], *Shuguang Deng* [a,*]

[a] School for Engineering of Matter, Transport and Energy, Arizona State University, Tempe, AZ, 85287, United States

[b] ASU LightWorks® and School of Sustainability, Arizona State University, Tempe, AZ, 85287-5402, United States

[c] ASU LightWorks® and School of Molecular Sciences, Arizona State University, Tempe, AZ, 85287-5402, United States

Corresponding author:

E-mail: shuguang.deng@asu.edu (S. Deng)

Abstract

In this work, we aimed to design, build, and evaluate an oxygen separation system to provide an inert sweep gas with low oxygen partial pressure (p_{O2}) to redox-active thermochemical energy conversion reactors for a range of applications, including two-step redox cycles for thermochemical energy storage, water splitting, and carbon-dioxide splitting. The separation is based on an oxygen-selective sorbent, $YBaCo_4O_{7+\delta}$ (YBC114), which has excellent oxygen sorption and desorption properties demonstrated in our previous work. The oxygen separation performance of YBC114 was comprehensively studied by thermogravimetric analysis, sorption breakthrough experiments, and temperature swing sorption - desorption cycles. The results reveal that YBC114 can produce inert sweep gas with an oxygen concentration of less than 100 ppmv for at least 20 minutes during the thermal swing adsorption (TSA) cycle with the current sorption bed configuration, and the performance is consistent from cycle to cycle. The optimal sorption and desorption temperatures for the TSA process with YBC114 are determined to be 300°C and 500°C, respectively. Although challenges remain for the current separation system (e.g., high sorption temperature and slow kinetics), this study demonstrates the potential to use the oxygen-selective sorbent to produce an inert sweep gas, the feasibility of the oxygen separation concept, and guides new sorbent material development to make this application economically practical. A simple procedure is described for designing the YBC114 oxygen separation process.

Keywords: YBC114, Oxygen separation, TSA, energy storage systems

1. Introduction

The increasing worldwide energy demand and global climate concerns necessitate technologies for producing renewable energy, such as concentrating solar power (CSP)[1]. On-demand electricity dispatchability, using an intermittent solar resource requires energy storage, such as thermochemical energy storage (TCES), such as storing energy in hot, reduced redox-active metal oxides[2–4]. TCES enables both significantly higher temperatures than current state-of-the-art CSP storage systems (e.g., molten salt storage)[5,6], and higher energy storage density, owing to the combined sensible and chemical storage[7]. High-temperature operation enables the use of high-efficiency power cycles. A storage scheme with higher power cycle efficiency and higher energy density could both decrease the cost of solar-derived electricity, and its value when dispatched on demand.

A key technical challenge and ongoing task in the practical implementation of redox-active metal oxide TCES is to create and maintain a low oxygen partial pressure (p_{O2}) during the charging step, which consists of heating and thermal reduction (TR). Low p_{O2} increases the reduction extent of the storage material for a given TR temperature. To lower the p_{O2}, current approaches use an inert sweep gas (ISG) or vacuum pumping. However, both approaches are energy-intensive and require large capital cost[8–11]. Oxygen separation is an attractive alternative for ISG purification due to its relatively low cost, flexible operation, and efficient regeneration[12]. Oxygen can be separated from the TR sweep gas (typically a mixture containing N_2 and O_2) with an oxygen-selective sorbent to produce ISG for TCES reactors. Ideally, the sorption and desorption (sorbent regeneration) can operate cyclically with multiple beds, so that the desired oxygen-depleted product gas is substantially continuous.

Oxygen-selective sorbent materials have been studied experimentally in previous work, such as CoO[8], silver salts[13], zeolites X[14,15], and perovskites ($SrFeO_{3-\delta}$[16], $CaCo_xZr_{1-x}O_{3-\delta}$[17], $La_{0.1}Sr_{0.9}Co_{0.9}Fe_{0.1}O_{3-\delta}$[18]). However, these materials have drawbacks: chemical instability, unacceptable adsorption properties, and/or high cost due to high temperatures for oxygen uptake and regeneration, limiting their suitability for the current oxygen separation application[13]. As a step toward the goal of low temperature and satisfactory oxygen sorption performance, we evaluated an oxygen ion conductor $YBaCo_4O_{7+\delta}$ (YBC114) for the oxygen separation application, due to its excellent oxygen uptake and release performance, and relatively low operating temperatures. YBC114 was initially reported by Valldor et al. in 2002[19], and has been studied for several potential applications such as oxygen storage material[20], oxygen sensor[21], and robust catalysts for H_2O_2 oxidation[22] and soot oxidation[23]. Due to its unique oxygen storage property, YBC114 has an infinitely large oxygen selectivity over nitrogen or other non-oxygen species. YBC114, for which we have data from our previous work[24], is capable of capturing O_2 within a narrow temperature range from 275 to 325°C and desorbing most of O_2 at a temperature higher than 400°C, due to its special crystal structure and the changeable valence of its Co ions. The sorption and regeneration temperatures are both much lower than other perovskites or redox-active metal oxides[25,26]. The equation below shows the reaction for sorption and desorption of O_2 on YBC114:

$$\frac{1}{\delta}YBaCo_4O_7 + \frac{1}{2}O_2 \leftrightarrow \frac{1}{\delta}YBaCo_4O_{7+\delta} \quad (1)$$

The sorbent material also shows consistent sorption and desorption performance during cycles, thus ideal for the temperature swing adsorption (TSA) process.

YBC114 is not without challenges. The oxygen separation process with YBC114 relies on the bulk transport of oxygen, which typically limits oxygen uptake rates. To address the challenge, Ermanoski and Stechel have proposed a chemisorption-based approach[27]. In this concept, the entirety of the oxygen adsorption occurs on a sorbent surface, at or around ambient temperatures. Desorption (activation) of the sorbent occurs at ~250-350°C. While exploring the desirable high surface area adsorbents for oxygen chemisorption, YBC114 is still an excellent baseline material for the conceptual design and preliminary performance testing of the oxygen separation system due to its known oxygen sorption properties. To address the kinetic limitations common in oxygen ion conductors, we prepared YBC114 with a sol-gel method (for smaller particle size) because the previous work[24] showed that the particle size has a significant effect on the oxygen sorption kinetics of YBC114. We initially studied the oxygen sorption and desorption properties of YBC114 with thermogravimetric analysis (TGA). We then designed and assembled an oxygen separation prototype with YBC114, and tested oxygen sorption performance with breakthrough and TSA experiments.

In the following sections, we will first describe the experimental methodology in Section 2, followed by the design of the oxygen separation system and preliminary performance testing results and discussion in Section 3. A conclusion is then drawn in the last section.

2. Experimental

The experimental section begins with the synthesis methods for YBC114. It will then illustrate the procedures of a series of experiments to test the oxygen sorption performance of YBC114 via TGA, fixed bed breakthrough experiments, and TSA operation.

2.1 Synthesis of YBC114

The YBC114 sample was synthesized with an ethylenediaminetetraacetic acid (EDTA) sol-gel method. Firstly, stoichiometric amounts of Y_2O_3 (Alfa Aesar, 99.995%), $Ba(NO_3)_2$ (Acros Organics, 99+%), $Co(NO_3)_2{\cdot}6H_2O$ (Sigma-Aldrich, 99+%) were mixed and dissolved in excess HNO_3 solution (Acros Organics, 68-70%), followed by the addition of EDTA (Honeywell, 99+%). The molar ratio of EDTA and all the metal ions (M^+) is 1.5:1. The solution was then neutralized with $NH_3{\cdot}H_2O$ (Thomas Scientific, 28% in water) until the pH of the solution was about 8. The solution was dried at a heating plate with stirring until it self-burned to fluffy ashes. The ashes were transferred to a muffle furnace and calcined at 1000°C in the air for 10 hours. After sintering, the resulting samples were cooled back to room temperature rapidly and milled.

2.2 Thermogravimetric measurement

A thermogravimetric analyzer (TGA, Netzsch TG 209 F1 Libra) was used to investigate the oxygen uptake and release characteristics. The mass of the sample for each measurement was 20-50 mg. All the samples were fully reduced at 400°C in 20 ml/min nitrogen flow for 2 hours before the measurements. The measurements were performed in a mixed gas flow of oxygen (Matheson, UHP) and nitrogen (Matheson, UHP). The p_{O2} was controlled by adjusting the ratio of oxygen and nitrogen in the mixed gas flow.

2.3 Breakthrough experiments

Figure 1 shows the schematic of the oxygen separation test prototype. We firstly prepared a sorption column packed with 20 g of YBC114 and 180 g of inert packing material (silica grain) and completed gas connections that allow counter-current gas flows for sorption and desorption. During the sorption step, a mixture of N_2 and O_2 flows through the sorption column by opening

V1 and V2. While in desorption, we switch to a counter-current purge gas flow by opening V3 and V4. A tube furnace controls the temperatures during sorption and desorption (Thermo Scientific Lindberg/Blue M). The oxygen concentration of the outlet stream for both sorption and desorption is measured and recorded by an oxygen analyzer (AII GPR-1500 GB) that has multiple ranges from 0-10 ppmv to 0-25% for flexible measurements.

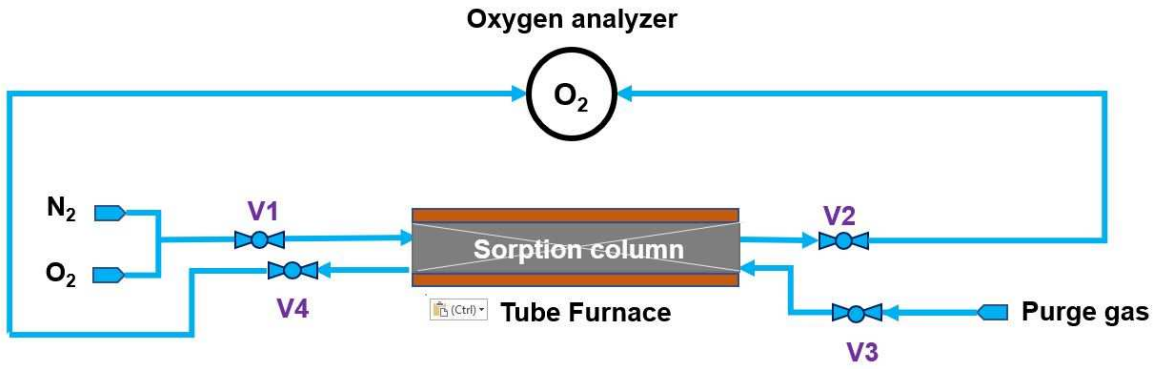

Figure 1. Schematic of the O_2 separation test prototype

2.4 TSA operation

For the TSA operation, we used the same oxygen separation prototype that was introduced previously. We first regenerate the sorption bed with N_2 for 24 hours, to remove the initial adsorbed O_2 content in the particles. We then start running the TSA cycles that include sorption, heating, desorption, and cooling. The operating procedures and conditions of each step in the TSA process are illustrated in Table 1.

Table 1. Operation procedure and conditions for TSA cycles

Step	Valve	Feed gas	Column temperature

Sorption	V_1, V_2	$O_2 + N_2$	275-325 °C
Heating	V_2		from 275-325 °C to 400-500 °C
Desorption	V_3, V_4	N_2, counter-current	400-500 °C
Cooling	V_4		from 400-500 °C to 275-325 °C

3. Results and discussion

To ensure the oxygen separation system is feasible and economical, a conceptual design of the oxygen separation system was first developed. Figure 2 shows the process flow diagram (PFD) of the oxygen separation design. The inlet of the sorption column connects to oxygen and inert gas, which mixes to mimic the reduction sweep gas coming out from the reduction reactor and other application systems. The feed gas flows through the sorption column for oxygen sorption and produces an ISG with low p_{O2}. We will include an inline gas heater to heat the feed stream before entering the sorption column, as well as a cooler to cool down the outlet stream for the protection of measurement components. For desorption, the sorbent material regenerates with a purge gas (e.g. air) at a higher temperature and is ready for sorption again. We can repeatedly change the temperatures of the sorbents for sorption-desorption cycles, which is a TSA operation.

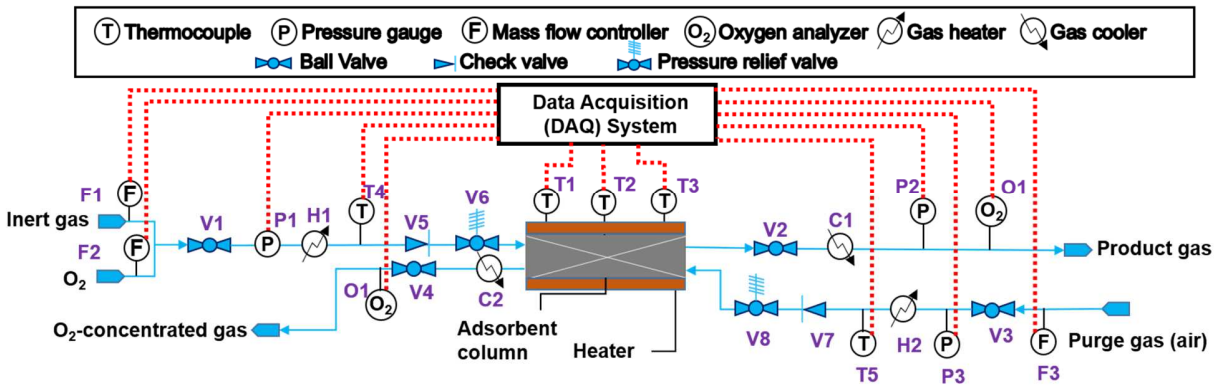

Figure 2. Process flow diagram of the O_2 separation design

The four-step TSA process includes sorption, heating, counter-current desorption, and cooling. Ideally, the TSA process would be carried out in a sorption system containing multiple sorption units in parallel, where one unit can be in sorption operation while other units are undergoing heating, desorption, or cooling. The sorption/desorption cycle is repeatedly carried out in a manner such that the production of the desired oxygen-depleted product is effectively continuous.

The properties we used for the adsorber design calculation include sorbent densities, void fractions, sorption isotherms, kinetics, and fixed bed dynamics. Since the system is intended to operate in TSA mode, we also did heat transfer modeling and optimized the column dimensions to minimize the thermal resistance from the heating source to the sorbent material. We performed a 1-D transient heat transfer calculation on the radial direction of the sorption bed, and the modeling equation is as follows.

$$\frac{dT}{dt} = \frac{k}{c\rho}\left(\frac{\partial^2 T}{\partial x^2}\right) \quad (2)$$

Where T is temperature, t is time, k is thermal conductivity, c is heat capacity, ρ is density, and x is the radial distance from the center of the pipe. Figure 3 shows the transient temperature

profiles during the heating and cooling steps (assuming forced air cooling) of a TSA cycle. The sorption and desorption temperatures are assumed to be 275 and 400°C. One can observe the major thermal resistance lies in the sorbent layer because the temperature difference in the pipe wall layer is insignificant. The overall sorption system can complete heating within 3 minutes, and cooling within 20 minutes.

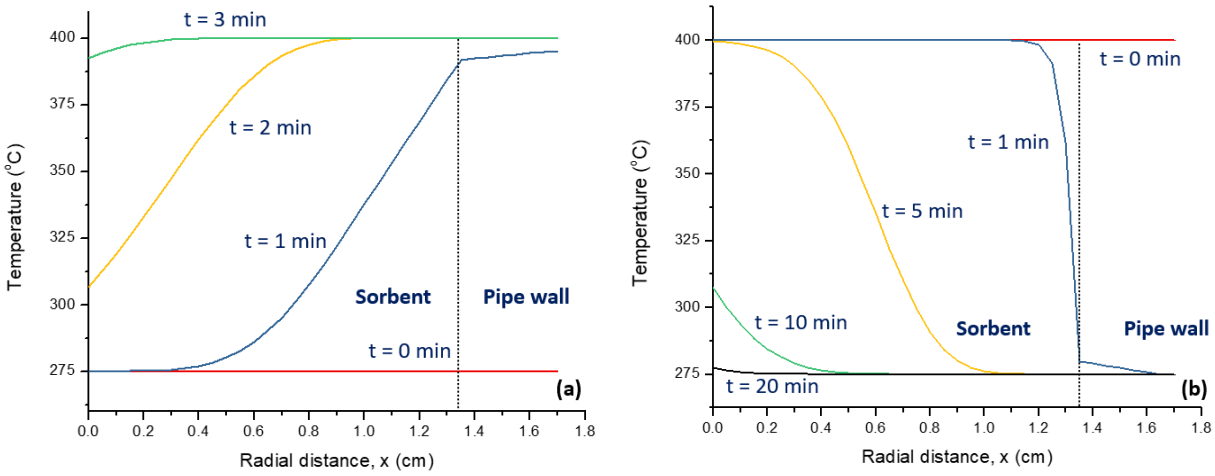

Figure 3. Temperature profiles during (a) heating and (b) cooling of the sorption bed

The baseline sorbent material used in the oxygen separation process is YBC114. To assess the oxygen sorption isotherms of YBC114 at different temperatures, we conducted the isotherm measurements at various p_{O2}s with TGA at 275, 300, and 325°C. We developed a Langmuir-like isotherm model (Sips model) to fit the experimental isotherm data for future process simulation. The equation of the isotherm model is as follows:

$$q = q_{sat}\frac{bp_{O2}{}^{n}}{1 + bp_{O2}{}^{n}} \quad (3)$$

Where q is the uptake amount, q_{sat} is the saturation uptake amount, b and n are isotherm constants. Values of q_{sat}, b, and n are determined with a non-linear regression model based on the

182 experimental isotherm data at different temperatures and summarized in Table 1. Figure 4 shows
183 a comparison between the experimental and simulated isotherm curves. One can observe that the
184 Sips model has an excellent fit to the experimental isotherm data, even for the low p_{O2} range that
185 is more applicable to the existing energy storage applications. Overall, YBC114 shows the
186 highest oxygen sorption capacities at 275°C, albeit quite close to 300°C when p_{O2} approached
187 100 kPa.

188 Table 2. Sips model parameters for oxygen sorption on YBC114

T (°C)	275	300	325
q_{sat} (mmol/g)	1.12	1.07	0.38
b (kPa^{-n})	0.142	0.047	0.110
n	0.87	1.20	0.99

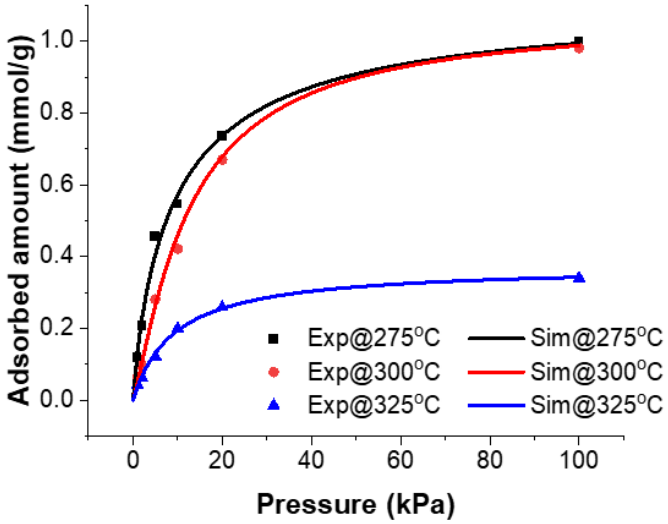

189

190 Figure 4. Experimental sorption isotherms and Sips fit of YBC114

191

To roughly estimate the working capacities in the TSA process, we repeated the isotherm measurement at 400°C (potential desorption temperature) and compared it with the isotherm profile at 275°C, as Figure 5 shows. The oxygen non-stoichiometry (δ) represents the amount of oxygen sorbed, which is the number of additional oxygen atoms per unit formula of YBC114. The working capacity between 275 and 400°C, at a p_{O2} of 21 kPa, is 0.45 mol O_2/mol YBC114 (δ = 0.9). The capacity is found to be higher than most reported oxygen-selective material like LSCF group perovskites (δ = 0.2-0.4)[28–30], SCF group perovskites (δ = 0.4-0.5)[31–33], and zeolite X (0.1-0.2 mmol/g, < 0.1 if converts to δ)[14], which is favorable. Figure 6 shows the temperature and mass change profiles of TSA cycles between 275 and 400°C evaluated with TGA. One can observe that YBC114 shows good cyclability for 10 TSA cycles, as we do not see any performance loss from cycle to cycle regarding the oxygen sorption performance of the material. YBC114 is therefore an excellent baseline sorbent material to be studied for the TSA process for oxygen separation.

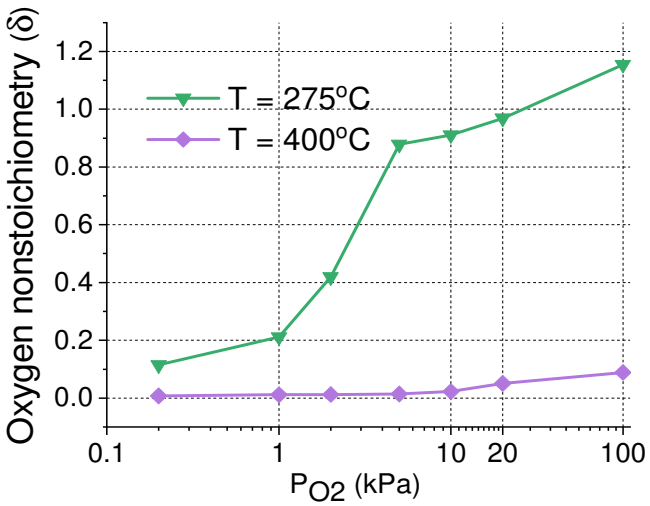

205

206 Figure 5. O_2 uptake isotherms of YBC114 at 275°C and 400°C

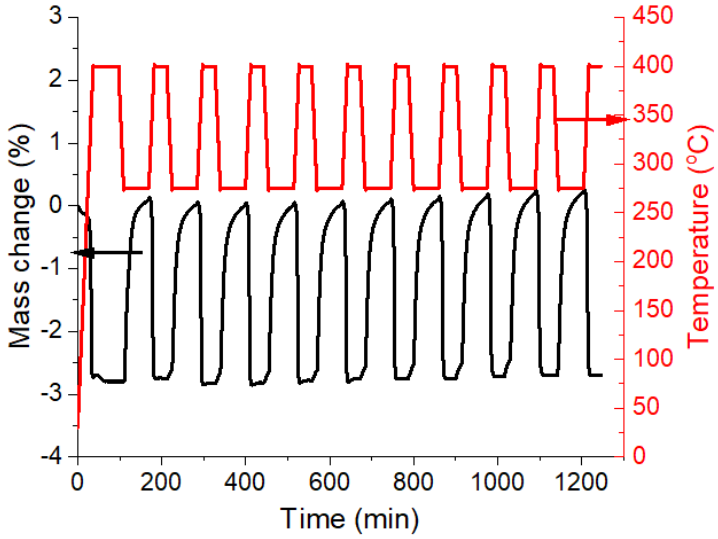

207

208 Figure 6. Temperature swing O_2 uptake-release cycles tested from TGA, p_{O2} = 21 kPa

209

210 After the design of the oxygen separation system and initial characterization of the material, we
211 assembled an oxygen separation lab prototype (Figure 1) for preliminary performance testing.
212 The lab prototype is a simplified version of the conceptual design, but sufficient for preliminary
213 sorption evaluations on the sorbent material. Before starting the oxygen sorption experiments in

214 the packed column, it is necessary to understand the role of pressure drop under various flow
215 conditions. A common concern when using small particles is the large column pressure drop that
216 could reduce process performance. To mitigate the potential risk of a high pressure drop, we mix
217 the sorbent material (particle size = 50-100 μm) with inert packing material (particle size = 1
218 mm) that has a larger particle size and then load the particle mixture to the sorption column.
219 Compared with the conventional separately packing method that locates sorbents in the middle
220 and inert material on the sides, the mixed packing method reduces the pressure drop to almost
221 one-eighth as shown in Figure 7. The values presented in this figure are experimentally measured.

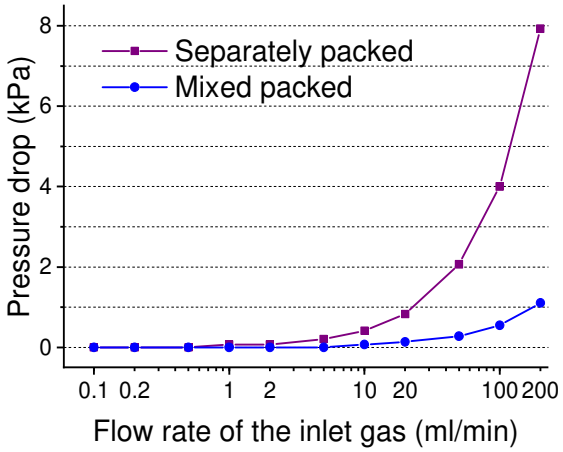

222

223 Figure 7. Pressure drop of the sorption column with two packing methods

224

225 After completion of the material packing and component connections, we start the oxygen
226 sorption breakthrough experiments with YBC114. The main performance characteristics we
227 focus on during breakthrough experiments is the outlet oxygen concentration profile of sorption
228 and desorption. A breakthrough occurs when the outlet oxygen concentration has a significant
229 increase during the sorption step (e.g., we defined a breakthrough that occurred when the outlet
230 oxygen concentration reached 100 ppmv). The shape of the breakthrough curve contains

information about the mass transfer properties of the sorption system. We can also determine the working capacity of the sorbent material for a dynamic sorption process by integrating the breakthrough data. Figure 8 shows the oxygen sorption breakthrough curves at 275, 300, and 325°C with 1% oxygen mixture. The results show that YBC114 produces an ISG for about 10 minutes at 275 and 325°C, and 20 minutes at 300°C. We found 300°C to be the optimum sorption temperature since it has the longest duration for producing an ISG. From our previous TGA characterizations[24], YBC114 has a larger oxygen sorption capacity at 275°C and a faster oxygen sorption rate at 300°C. Combined capacity and kinetics can account for the improved process performance at 300°C. We also performed breakthrough simulations with the isotherm data obtained from TGA characterizations and inferred mass transfer coefficients from sorption breakthrough measurements. The simulated results match the experimental data well.

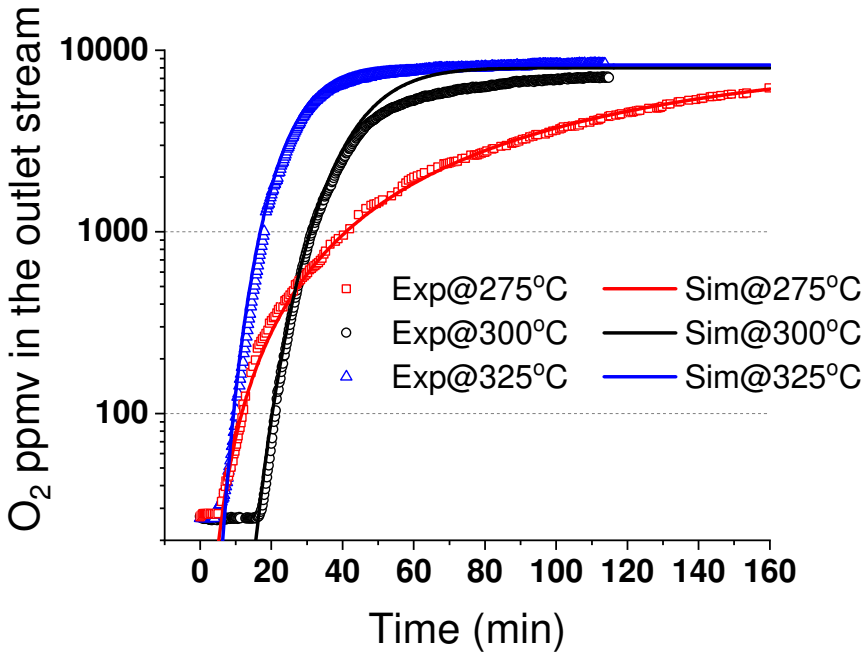

Figure 8. Experimental and simulated O_2 Sorption breakthrough curve

To study the effect of desorption temperature, we performed three consecutive sorption-desorption cycles with identical sorption conditions but different desorption temperatures from 400 to 500°C. As shown in Figure 9, the desorption profile at 500°C has a narrower and higher peak than the first two cycles, which indicates a faster desorption rate. Desorption kinetics is crucial for the overall efficiency of producing ISG with TSA cycles since fast desorption shortens the minimum duration required for desorption in each cycle. 500°C is therefore the preferred desorption temperature in this scenario. Certainly, desorption at higher temperatures can further shorten the desorption step duration. Higher desorption temperatures require more thermal energy consumption and a longer duration for heating and cooling steps. An optimum desorption temperature can only be obtained by process optimization with specific optimization targets (minimal capital investment, least energy consumption, etc.).

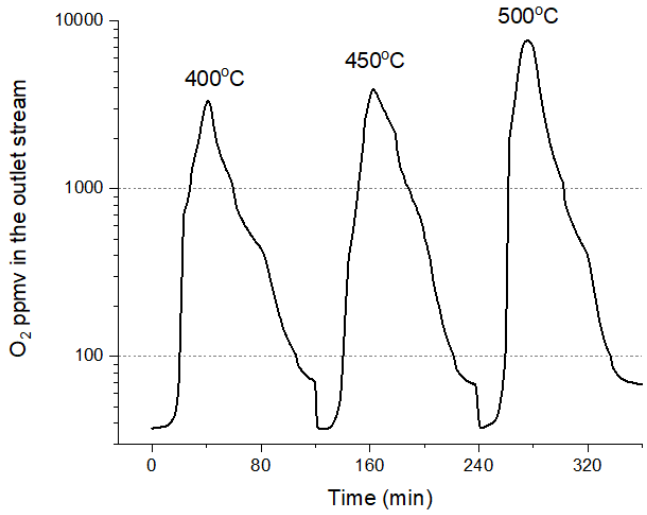

Figure 9. Desorption profiles of YBC114 at varying desorption temperatures

To fully assess the effect of other operating variables except for temperatures (such as p_{O2} and flow rate) on process performance, we performed a series of breakthrough experiments with

varying oxygen concentrations or flow rates. The sorption and desorption temperatures are fixed at 300°C and 500°C, respectively. Table 2 summarizes oxygen sorption performance at different p_{O2}s or flow rates. We measured the static capacity in previous TGA characterizations, and we obtained the dynamic capacity from the oxygen sorption breakthrough experiments. We also estimated the mass transfer coefficients for different p_{O2}s with a linear driving force (LDF) model that typically has a good kinetics prediction of cyclic sorption systems. The equation of the LDF model is as follows:

$$\frac{\partial q}{\partial t} = k(q_{sat} - q) \tag{4}$$

Where k is a lumped mass transfer coefficient that includes all the mass transfer mechanisms during fixed-bed sorption, and q_{sat} is the saturation uptake amount that is determined from the isotherm model. As evident in the table, both capacities and mass transfer coefficients increase with p_{O2}, while the breakthrough time decreases with p_{O2}. As for the effect of flow rate, the sorption capacity inferred from breakthrough data at different flow rates are close, and all of them are less than the static oxygen capacity, which would be expected due to the existence of a mass transfer zone in the fixed bed. The breakthrough time and pressure drop also show reasonable correlations with the flow rate as the trend is within our expectations.

Table 3. Summary of O_2 sorption performance of YBC114 at different p_{O2}s or flow rates

Effect of p_{O2} (flow rate = 100 ml/min, superficial velocity = 27.32 cm/min)				
O_2 concentration (%)	Static O_2 capacity (mol O/mol YBC114)	Dynamic O_2 capacity (mol O/mol YBC114)	Breakthrough time (min)	Mass transfer coefficient (1/s)
1	0.075	0.055	42	0.02

5	0.32	0.24	35	0.17
10	0.48	0.35	24	0.25
30	0.85	0.46	11	0.44
Effect of flow rate (O_2 concentration = 10%)				
Flow rate (ml/min)	Static O_2 capacity (mol O/mol YBC114)	Dynamic O_2 capacity (mol O/mol YBC114)	Breakthrough time (min)	Pressure drop (kPa)
50	0.48	0.34	50	4.2
100		0.35	23	9.4
200		0.37	11	20.1

To further investigate the performance of the oxygen separation unit with YBC114, we performed a TSA operation with the same setup used in the breakthrough experiments. In this process, we first regenerate the sorption bed with N_2 at 500°C for 24 hours, to remove the initial sorbed oxygen content in the particles. We then cool the temperature to 275°C for sorption, switch the flow to a mixture of N_2 and O_2 with a p_{O2} of 10 kPa (i.e., 10% O_2). For the next cycle, we repeat the TSA between 300 and 500°C for sorption and desorption. Figure 10 shows the oxygen concentration profile for the first three cycles. Each cycle takes two hours, which includes 20 minutes sorption, 20 minutes heating, 40 minutes desorption, and 40 minutes cooling. The key parameter of interest here is the duration for producing an ISG that has an oxygen concentration lower than 100 ppmv in the sorption step in each cycle. As evident in the plot, the O_2 concentration during the whole sorption step during the three cycles (shown as valleys of the curve) is less than 100 ppmv (equivalent to an inert concentration > 99.99%) without an obvious increase from cycle to cycle. The TSA results are consistent with previous breakthrough measurements. The purity of the ISG product is much higher than most conventional vacuum pressure swing adsorption (VPSA) processes for oxygen removal with zeolite materials, which

typically produce nitrogen with a purity of 95-99.5%[34–36] (albeit ultra-high purity might be achievable with much higher energy cost due to the deep vacuum).

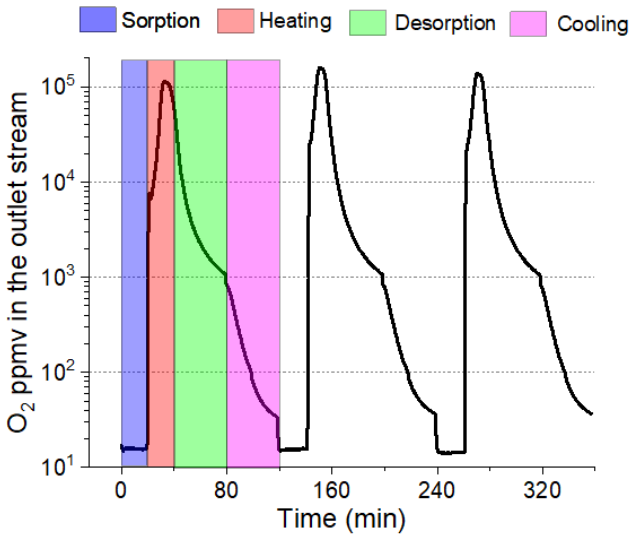

Figure 10. O_2 concentration profile during TSA cycles at sorption temperature of 300°C

We performed process simulations to simulate the TSA operation between 300°C and 500°C with a feed mixture containing 1% or 10% oxygen. The simulation model is based on the isotherm data obtained from the TGA characterizations and the mass transfer coefficients inferred from sorption breakthrough measurements. The TSA process is simulated for 20 cycles to verify if it reached a cyclic steady state. As shown in Figure 11, the oxygen concentration profiles under both feed conditions (1% and 10% oxygen) were reasonably consistent from cycle to cycle showing a similar trend. When we compare the peak values of each cyclic oxygen concentration curve, we find they initially decrease and gradually stabilize. For example, the decreasing rate during the first five cycles is in a range of 1-2%. For the last five cycles (i.e., cycles 16-20), the decreasing rate reduces to less than 0.2%; hence, the TSA process has reached the cyclic steady state.

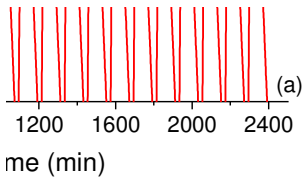

309 Figure 11. Simulated TSA profile operated between 300°C and 500°C with (a) 1% O_2 and (b)

310 10% O_2

311

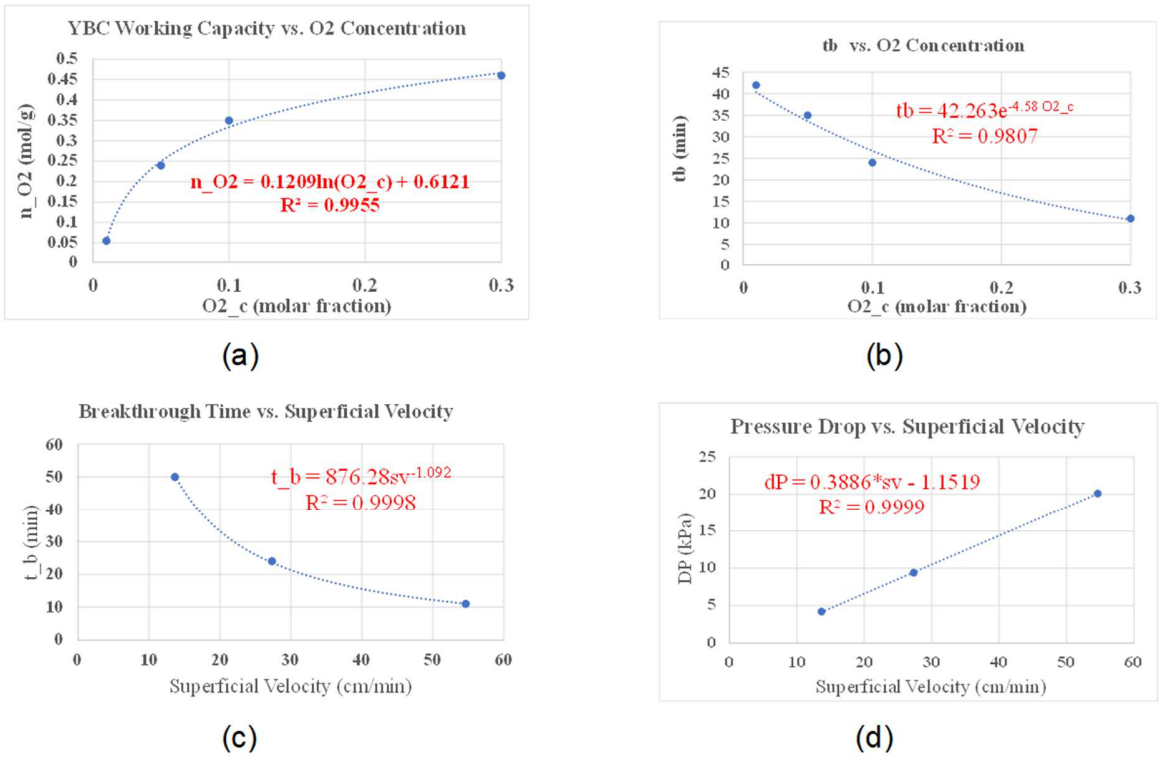

312

313 Figure 12. Summary of YBC114 O_2 adsorption process design equations (a) effect of O_2

314 concentration on working capacity; (b) effect of O_2 concentration on adsorption breakthrough

315 time; (c) effect of superficial velocity on adsorption breakthrough time; (d) effect of
316 superficial velocity on pressure drop.
317

318 From the design data (Table 2), we have developed four design equations for the YBC114 based
319 oxygen separation system, which Figure 12 shows. The design for the YBC114 O_2 separation
320 system involves the following steps: (1) calculate adsorbent working capacity from the oxygen
321 feed concentration by using Figure 12(a); (2) determine adsorption breakthrough time using both
322 Figure 12 (b) and Figure 12 (c), and the smaller value is selected; (3) calculate the sorbent
323 (YBC114) mass requirement by a simple mass balance equation assuming the YBC114 sorbent
324 captures all oxygen in the feed gas stream. Because the experiments were conducted with 20%
325 YBC114 powder (100 μm particle size) mixed with 80% silica beads (1 mm) to avoid an
326 excessive pressure drop, the mass of silica beads can be determined; (4) calculate the sorbent
327 volume by dividing the sorbent mass with packing density of the mixed adsorbent. (5) determine
328 the sorption configuration after selecting the sorption step's superficial velocity. Also calculate
329 the sorption inner diameter, sorbent packing height, and sorption mass; (6) determine the
330 pressure drop for the actual adsorber configuration using Figure 12(d); (7) calculate the moles of
331 oxygen atoms sorbed by the sorbent. Although the adsorption cycle has been optimized for
332 different operating conditions, Figure 13 shows our suggested configuration and that is to use a
333 4-bed thermal swing adsorption system to perform the YBC114 O_2 separation. The 4-bed system
334 enables a direct heat exchange between the heating and cooling gas streams at the same time
335 without using gas storage tanks; (8) given the adsorption system, calculate the energy
336 consumption for overcoming the pressure drops, replenishing the heat of adsorption and thermal

energy loss during the heat-exchange. The entire design process can be carried out in MATLAB by programming all the equations and calculation steps in a MATLAB function m-file.

4-Bed System				
Step Duration	Bed - 1	Bed - 2	Bed - 3	Bed - 4
0-1	Adsorption	Heating	Desorption	Cooling
1-2	Heating	Desorption	Cooling	Adsorption
2-3	Desorption	Cooling	Adsorption	Heating
3-4	Cooling	Adsorption	Heating	Desorption

Figure 13. Cyclic step arrangement for 4-bed thermal swing adsorption system

4. Conclusion

An oxygen separation system was designed to produce an ISG with low p_{O2} via the TSA process. The performance of the oxygen separation system was evaluated with the baseline material, YBC114, which has a large oxygen uptake capacity in a medium temperature range. YBC114 shows good cyclability with decent oxygen working capacity (0.45 mol O_2/mol YBC114) from TGA characterizations. With the oxygen separation lab prototype, we identified that the optimal sorption and desorption temperatures for the TSA process with YBC114 are 300°C and 500°C, respectively. The effects of oxygen concentration and gas flow rate on the oxygen sorption performance were also assessed to design and optimize the operational parameters of the TSA process. We also demonstrated that YBC114 can produce an ISG with an oxygen concentration less than 100 ppmv for at least 20 minutes during a TSA cycle (for the given configuration), and the performance is consistent from cycle to cycle.

Overall, the results from preliminary performance testing of the oxygen separation prototype with YBC114 are satisfactory and within our expectations. The results have shown the potential to use YBC114 as the sorbent to produce an ISG and demonstrated the feasibility of the oxygen separation concept. Nevertheless, challenges remain before the system could advance to commercialization; for example, the kinetic rate of oxygen uptake should be faster, and ideally, the uptake temperature lower, while maintaining a similar change in temperature between sorption and desorption. Research in further material development would be required to advance this application to economic practicality. A design procedure was developed for designing the YBC114 oxygen separation system.

Acknowledgment

This material is based upon work supported by the U.S. Department of Energy's Office of Energy Efficiency and Renewable Energy (EERE) under the Solar Energy Technologies Office Award Number DE-EE0008991. We also extend our gratitude to Mr. Yixin Liu for helping with the sorbent material synthesis. We are thankful to Prof. Christopher Muhich of Arizona State University for the valuable suggestions on this research.

Reference

1. He, Y. L. *et al.* Perspective of concentrating solar power. *Energy* **198**, 117373 (2020).

2. Steinfeld, A. & Palumbo, R. Solar Thermochemical Process Technology. in *Encyclopedia of Physical Science and Technology* 237–256 (2003). doi:10.1016/b0-12-227410-5/00698-0

3. Pardo, P. *et al.* A review on high temperature thermochemical heat energy storage. *Renewable and Sustainable Energy Reviews* **32**, 591–610 (2014).

4. Tescari, S. *et al.* Thermochemical solar energy storage via redox oxides: Materials and reactor/heat exchanger concepts. in *Energy Procedia* **49**, 1034–1043 (2014).

5. Wu, Y. ting, Ren, N., Wang, T. & Ma, C. fang. Experimental study on optimized composition of mixed carbonate salt for sensible heat storage in solar thermal power plant. *Sol. Energy* **85**, 1957–1966 (2011).

6. Carrillo, A. J. *et al.* Thermochemical energy storage at high temperature via redox cycles of Mn and Co oxides: Pure oxides versus mixed ones. *Sol. Energy Mater. Sol. Cells* **123**, 47–57 (2014).

7. AuYeung, N. & Kreider, P. Solar thermochemical energy storage. *Chem. Eng. Prog.* **113**, (2017).

8. Brendelberger, S., von Storch, H., Bulfin, B. & Sattler, C. Vacuum pumping options for application in solar thermochemical redox cycles – Assessment of mechanical-, jet- and thermochemical pumping systems. *Sol. Energy* **141**, 91–102 (2017).

9. Sivadas, D. L., Vijayan, S., Rajeev, R., Ninan, K. N. & Prabhakaran, K. Nitrogen-enriched microporous carbon derived from sucrose and urea with superior CO2 capture performance. *Carbon N. Y.* **109**, 7–18 (2016).

10. Brendelberger, S., Roeb, M., Lange, M. & Sattler, C. Counter flow sweep gas demand for the ceria redox cycle. *Sol. Energy* **122**, 1011–1022 (2015).

11. Lin, M. & Haussener, S. Solar fuel processing efficiency for ceria redox cycling using alternative oxygen partial pressure reduction methods. *Energy* **88**, 667–679 (2015).

12. Arias, B. *et al.* Emerging CO2 capture systems. *Int. J. Greenh. Gas Control* **40**, 126–166 (2015).

13. Jayaraman, A. & Yang, R. T. Stable oxygen-selective sorbents for air separation. *Chem. Eng. Sci.* **60**, 625–634 (2005).

14. Jayaraman, A., Yang, R. T., Cho, S. H., Bhat, T. S. G. & Choudary, V. N. Adsorption of nitrogen, oxygen and argon on Na-CeX zeolites. *Adsorption* **8**, 271–278 (2002).

15. Peter, S. A., Moharir, A. S. & Jasra, R. V. Selective adsorption of oxygen over argon in alkaline-earth-metal cation-exchanged zeolite X. *Ind. Eng. Chem. Res.* **49**, 7524–7529 (2010).

16. Brendelberger, S., Vieten, J., Vidyasagar, M. J., Roeb, M. & Sattler, C. Demonstration of thermochemical oxygen pumping for atmosphere control in reduction reactions. *Sol. Energy* **170**, 273–279 (2018).

17. Zheng, Q., Lail, M., Zhou, S. & Chung, C. C. CaCoxZr1−xO3−δ Perovskites as Oxygen-Selective Sorbents for Air Separation. *ChemSusChem* **12**, 2598–2604 (2019).

18. Xu, M., Wu, H. C., Lin, Y. S. & Deng, S. Simulation and optimization of pressure swing adsorption process for high-temperature air separation by perovskite sorbents. *Chem. Eng. J.* **354**, 62–74 (2018).

19. Valldor, M. & Andersson, M. The structure of the new compound YBaCo4O7 with a magnetic feature. *Solid State Sci.* **4**, 923–931 (2002).

20. Parkkima, O., Yamauchi, H. & Karppinen, M. Oxygen Storage Capacity and Phase Stability of Variously Substituted YBaCo4O7+δ. *Chem. Mater.* **25**, 599–604 (2013).

21. Măicăneanu, A. *et al.* Organics removal from aqueous solutions using suspended and immobilized Romanian bentonites. *Stud. Univ. Babes-Bolyai Chem.* 82–93 (2011).

22. Parkkima, O., Silvestre-Albero, A., Silvestre-Albero, J. & Karppinen, M. Oxygen-Nonstoichiometric YBaCo4O7+δ as a Catalyst in H2O2 Oxidation of Cyclohexene. *Catal. Letters* **145**, 576–582 (2015).

23. Tian, G. *et al.* An oxygen pool from YBaCo4O7-based oxides for soot combustion. *Catal. Sci. Technol.* **6**, 4511–4515 (2016).

24. Xu, M., Ermanoski, I., Stechel, E. B. & Deng, S. Oxygen pumping characteristics of $YBaCo_4O_{7+\delta}$ for solar thermochemical cycles. *Chem. Eng. J.* **389**, 124026 (2020).

25. Agrafiotis, C., Roeb, M. & Sattler, C. Cobalt oxide-based structured thermochemical reactors/heat exchangers for solar thermal energy storage in concentrated solar power plants. in *ASME 2014 8th International Conference on Energy Sustainability, ES 2014 Collocated with the ASME 2014 12th International Conference on Fuel Cell Science,*

Engineering and Technology **1**, (Web Portal ASME (American Society of Mechanical Engineers), 2014).

26. Vieten, J. *et al.* Perovskite oxides for application in thermochemical air separation and oxygen storage. *J. Mater. Chem. A* **4**, 13652–13659 (2016).

27. Ermanoski, Ivan; Stechel, E. Thermally Driven Adsorption/Desorption Cycle for Oxygen Pumping in Thermochemical Fuel Production. *Solar Energy* **198(7)**,578-585 (2020) *DOI:10.1016/j.solener.2020.01.050*

28. Yang, Q., Lin, Y. S. & Bülow, M. High temperature sorption separation of air for producing oxygen-enriched CO2 stream. *AIChE J.* (2006). doi:10.1002/aic.10638

29. Yang, Z., Lin, Y. S. & Zeng, Y. High-temperature sorption process for air separation and oxygen removal. *Ind. Eng. Chem. Res.* (2002). doi:10.1021/ie010736k

30. Yang, Z. H. & Lin, Y. S. High-temperature oxygen sorption in a fixed bed packed with perovskite-type ceramic sorbents. *Ind. Eng. Chem. Res.* (2003). doi:10.1021/ie030313d

31. Rui, Z., Ding, J., Li, Y. & Lin, Y. S. SrCo0.8Fe0.2O3-δ sorbent for high-temperature production of oxygen-enriched carbon dioxide stream. *Fuel* (2010). doi:10.1016/j.fuel.2009.10.024

32. Yin, Q., Kniep, J. & Lin, Y. S. Oxygen sorption and desorption properties of Sr-Co-Fe oxide. *Chem. Eng. Sci.* **63**, 2211–2218 (2008).

33. Hao, P., Shi, Y., Li, S. & Liang, S. Oxygen sorption/desorption kinetics of SrCo0.8Fe0.2O3−δperovskite adsorbent for high temperature air separation. *Adsorption* **24**, 65–71 (2018).

34. Shokroo, E. J. Comparison of Two Pressure Swing Adsorption Processes for Air Separation Using Zeolite 5A and Zeolite 13X.

35. Steven P. Reynolds, Armin D. Ebner, and & Ritter*, J. A. Enriching PSA Cycle for the Production of Nitrogen from Air. *Ind. Eng. Chem. Res.* **45**, 3256–3264 (2006).

36. Ferreira, D., Boaventura, M., Bárcia, P., Whitley, R. D. & Mendes, A. Two-Stage Vacuum Pressure Swing Adsorption Using AgLiLSX Zeolite for Producing 99.5+% Oxygen from Air. *Ind. Eng. Chem. Res.* **55**, 722–736 (2016).

Graphical abstract

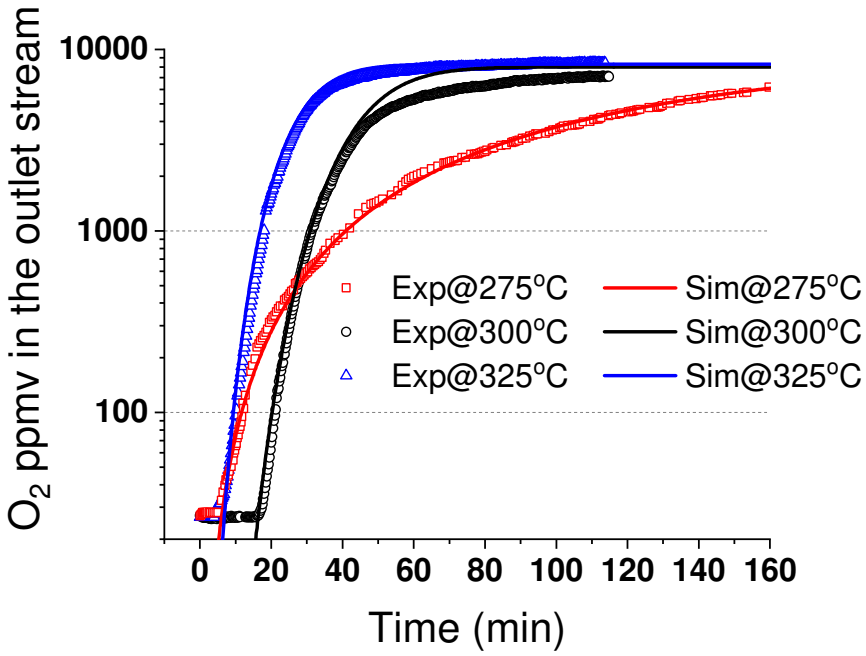

Experimental and simulated O_2 sorption breakthrough curves at different temperatures